This is a preprint, the final version is subject to change, of the American Mineralogist (MSA)
Cite as Authors (Year) Title. American Mineralogist, in press.
(DOI will not work until issue is live.) DOI: http://dx.doi.org/10.2138/am-2017-6033

Revision 2

Phase transition in SiC from zinc-blende to rock-salt structure and implications for carbon-rich extrasolar planets

YUTO KIDOKORO[1,2,*], KOICHIRO UMEMOTO[2], KEI HIROSE[2], AND YASUO OHISHI[3]

[1]Department of Earth and Planetary Sciences, Tokyo Institute of Technology, 2-12-1 Ookayama, Meguro, Tokyo 152-8551, Japan

[2]Earth-Life Science Institute, Tokyo Institute of Technology, 2-12-1 Ookayama, Meguro, Tokyo 152-8550, Japan

[3]Japan Synchrotron Radiation Research Institute, SPring-8, 1-1-1 Kouto, Sayo, Hyogo 679-5198, Japan

*E-mail: kidokoro.y.aa@m.titech.ac.jp

ABSTRACT

We have investigated the phase transition in SiC between the zinc-blende and rock-salt structures at high pressure and temperature in a laser-heated diamond-anvil cell. Results demonstrate that the transition occurs at 74 GPa and 2100 K with a 21 % density increase, reflecting the coordination number rising from four to six. In addition, our *ab initio* calculations show that the boundary has a negative Clapeyron slope of -4.0 MPa/K at 2000 K. The experimentally-determined phase boundary is located between those predicted by GGA and B3LYP functional. This transition may take place inside carbon-rich extrasolar planets, forming a boundary with a large density jump. Since SiC is rigid and highly thermally conductive, thermal convection in an SiC-dominant layer is not likely to occur. Nevertheless, the convection may be possible if planet interiors include both silicon carbide and silicate, and in this case the phase transition could affect the style of thermal convection.

Keywords: Silicon carbide, phase transition, zinc blende, rock salt, Clapeyron slope, extrasolar planet

INTRODUCTION

34 It is known that host stars of observed extrasolar planetary systems exhibit a wide
35 range of C/O elemental ratios from 0.3 to 1.9 (Bond et al. 2010). The condensation
36 models examined by Bond and others show that planets inside the snow line dominantly
37 consist of silicon carbide and carbon when the C/O ratio is greater than 0.8. The
38 super-Earth 55 Cancri e, a member of a known five-planet system and closest to its host
39 star, may be such a carbon-rich planet considering the host star's C/O value of 1.12.
40 Madhusudhan et al. (2012) demonstrated on the basis of observed mass–radius relation
41 that the interior of 55 Cancri e can be composed of layers of carbon, silicon carbide, and
42 iron.

43 SiC has attracted attention in a wide range of fields because of its strong fire
44 resistance, durability, etc. There are a variety of polytypes with cubic 3*C* (space group:
45 F-43m) and hexagonal 6*H* ($P6_3mc$) as common structures (numbers represent the
46 number of layers within a single stack). Pressure-induced phase transition has been
47 examined with both theory and experiment. Calculations under static conditions have
48 predicted the phase transformation between 3*C* (zinc-blende, ZB, -type) and rock-salt
49 (RS)-type structures (space group: Fm-3m) at 64.9–66.6 GPa (Figure 1) by local-density
50 approximation (LDA) (Chang and Cohen 1987; Karch et al. 1996; Sarasamak et al.
51 2008) and at 92 GPa by B3LYP functional (Catti 2001). Such a ZB–RS transition was

52 confirmed by experiments at a higher pressure range. The room-temperature
53 diamond-anvil cell (DAC) measurements by Yoshida et al. (1993) reported the transition
54 at 100 GPa. Sekine and Kobayashi (1997) demonstrated a solid–solid transition at 105 ±
55 4 GPa along Hugoniot compression. The recent *ab initio* calculations by Wilson and
56 Militzer (2014) predicted the phase transition from the RS to the *Cmcm* structure above
57 27 Mbar.

58 Here we carried out static high-pressure and -temperature (*P*-*T*) experiments to
59 constrain the ZB–RS transition boundary in a laser-heated DAC. We also performed *ab*
60 *initio* calculations to determine the transition pressure and its Clapeyron slope. These
61 results show that the phase transition occurs around 70 GPa with a high negative
62 Clapeyron slope and a significant volume change. Such ZB–RS transition in SiC forms
63 an important boundary with a large density jump, although it was previously not
64 considered in the interior model of 55 Cancri e (Madhusudhan et al. 2012).

65

66 **METHODS**

67 **High-pressure experiments**

68 High *P*-*T* conditions were generated in a laser-heated DAC. Diamond anvils with

beveled 150 μm or flat 300 μm culet were used. The starting material was a fine powder of hexagonal polytype of SiC (6*H*) from *Good Fellow* (>99% purity), whose grain size was 0.5–1.0 μm. A sample was pelletized, and coated with a gold film on both sides, which served as both a pressure standard and a laser absorber. We employed NaCl, KCl, or SiO_2 glass as a pressure medium. The SiC sample and the pressure medium were loaded into a 40–120 μm hole made in the center of a pre-indented rhenium gasket. After loading, a whole DAC was dried in a vacuum oven at 423 K for more than 12 hrs in order to avoid contamination by water. When removed from the oven, dry argon was introduced and we compressed the sample in an Ar atmosphere.

Sample heating and synchrotron X-ray diffraction (XRD) measurements were carried out at the BL10XU, SPring-8. The sample was heated from both sides of the DAC by using a couple of 100 W single-mode Yb fiber lasers with beam-shaping optics. A laser-heated spot was approximately 30 μm in diameter. We measured the temperature using a spectroradiometric method (Ozawa et al. 2016). Since an incident X-ray beam (wavelength 0.4131–0.4154 Å) was collimated to 6 μm in diameter at full width of half maximum, experimental temperature reported in Table 1 was the average in the 6 μm area of a hot spot.

Angle-dispersive XRD spectra of the sample were collected on a flat panel detector (*Perkin Elmer*) at high *P-T* during heating, and at high-*P*/room-*T* before and after heating. Exposure time was 1 sec. The two-dimensional diffraction signal was integrated into a one-dimensional pattern as a function of two-theta by using the IP analyzer software package (Seto et al. 2010). For the determination of phase transition boundary at high *P-T*, pressure at high temperature was obtained on the basis of the unit-cell volume of Au and its *P-V-T* equation of state (EoS) proposed by Fei et al. (2007). The uncertainty in pressure at high temperature is derived from errors in temperature during heating (±10%) and the volume of Au. For volume measurements at room-*T*, on the other hand, NaCl was used as a pressure marker because the XRD peaks of Au were sometimes masked when the sample included a large amount of RS-type SiC. The EoS of B2 NaCl determined by Sata et al. (2002) gives pressure consistent with that of Fei et al.'s EoS of Au at relevant high pressure and 300 K (Sata et al. 2010).

Ab initio calculations

Our *ab initio* calculations used the Perdew-Burke-Ernzerhof (PBE) form (Perdew et al. 1996) of generalized-gradient approximation (GGA) and the Perdew-Zunger (PZ) form (Perdew and Zunger 1981) of LDA for the exchange and correlation (XC)

functional. Vanderbilt's type pseudopotentials were used (Vanderbilt 1990). The cutoff radii for C and Si were 0.690 and 0.847 Å, respectively. A plane-wave basis set with a cutoff energy of 40 Ry was used. The **k**-point mesh was 8×8×8. We used the quasi-harmonic approximation to take phonon effects into account (Wallace 1972). Dynamical matrices were computed at the 4×4×4 **q**-point mesh using the density-functional-perturbation theory (Giannozzi et al. 1991; Baroni et al. 2001). Vibrational densities of states were obtained by interpolation of phonon frequencies on the 24×24×24 **q**-point mesh. All calculations were performed using the Quantum-ESPRESSO package (Giannozzi et al. 2009).

RESULTS

Phase transition in SiC

Six separate high *P*-*T* runs were performed with a gold pressure marker in a pressure range from 59 to 92 GPa (Table 1). After experiments, we recovered some samples from a DAC and examined their cross sections using a focused ion beam (FIB) system and a field-emission-type energy-dispersive spectroscopy (EDS). Dissociation of the SiC sample nor chemical reaction with a pressure medium was not observed.

Upon heating, the original 6*H*-type SiC underwent a phase transition either to ZB- or RS-type phase. In the first run, all sample peaks found at 56 GPa and 300 K were from the 6*H* phase (starting material) (Figure 2a, f). Upon heating to 2060 K at 68 GPa, the ZB 111 and 220 lines that overlap with the 012 and 110 peaks from 6*H*, respectively, became stronger and dotty (Figure 2b, g), indicating the phase transformation and grain growth of the ZB phase. After further compression at 300 K, all sample peaks were again from 6*H* at 67 GPa (Figure 2c). No new peaks were observed during heating to 2200 K for 2 min. The peaks from RS-type SiC first appeared at 92 GPa and 2610 K (Figure 2d). These new peaks grew, while those of 6*H* SiC further diminished when we reheated at 91 GPa and 2590 K (Figure 2e). In run #2, we first synthesized RS-type SiC during heating at 86 GPa and 2690 K in 12 min. The RS peaks grew upon further heating at 85 GPa and 2250 K for 23 min. It was then decompressed to 52 GPa at room temperature and reheated. The ZB-type phase appeared in 6 min, while the peaks from the RS-type phase diminished, at 59 GPa and 1640 K. Such a transition from RS- to ZB-type phase was observed also at 63 GPa and 1960 K.

Similarly in another four runs, the stabilities of the ZB and RS phases were determined using the following three criteria; 1) the appearance of new diffraction peaks, 2) grain growth inferred from spotty peaks in two-dimensional XRD image, and 3)

139 growth and reduction of the relevant peaks when both phases coexisted in the XRD
140 pattern. All of these results are summarized in Figure 3. The phase transition boundary
141 is located at 74 GPa and 2100 K.

142 On the other hand, our calculations show the static GGA and LDA ZB–RS transition
143 pressure to be 67 and 63 GPa, respectively, which is consistent with earlier LDA
144 calculations (64.9–66.6 GPa) (Chang and Cohen 1987; Karch et al. 1996; Sarasamak et
145 al. 2008). The GGA transition pressure is marginally higher than LDA. Across the
146 transition from ZB to RS, Si–C bond length increases from 1.771 Å to 1.915 Å at 67
147 GPa (static GGA), although the volume decreases by 17.9 %. It is due to the increase in
148 coordination number from four to six. Since the bond length increases, average phonon
149 frequency decreases. Hence the zero-point motion energy in the RS phase is lower than
150 that in the ZB phase. The transition pressure at 0 K with the zero-point motion is 65
151 GPa by GGA and 61 GPa by LDA, slightly lower than static transition pressure. Since
152 lower phonon frequencies give rise to higher vibrational entropy, the RS phase has a
153 wider stability field at higher temperature and the phase boundary has a negative
154 Clapeyron slope; the transition pressure at 2100 K is 60 GPa by GGA and 57 GPa by
155 LDA (Figure 3).
156

This is a preprint, the final version is subject to change, of the American Mineralogist (MSA)
Cite as Authors (Year) Title. American Mineralogist, in press.
(DOI will not work until issue is live.) DOI: http://dx.doi.org/10.2138/am-2017-6033

157 **Compression of SiC**

158 We measured sample volumes (V) at room temperature using NaCl as a pressure
159 standard between 57 and 78 GPa for the ZB phase and between 50 and 98 GPa for the
160 RS phase (Table 2). All of these data were collected after heating or thermal annealing.
161 We used the ZB 111 and 220 peaks and the RS 200 and 220 peaks to obtain their
162 unit-cell volumes. We fit the third-order Birch-Murnaghan EoS to the P-V data for the
163 RS SiC (Figure 4);

164 $$P(\mathrm{V}) = \frac{3}{2}K_0\left(\frac{V_0}{V}\right)^{\frac{5}{3}}\left[\left(\frac{V_0}{V}\right)^{\frac{2}{3}} - 1\right]\left[1 + \frac{3}{4}(K' - 4)\left\{\left(\frac{V_0}{V}\right)^{\frac{2}{3}} - 1\right\}\right] \quad (1)$$

165 The fitting gives V_0 = 10.2(1) cm^3/mol and bulk modulus K_0 = 235(9) GPa (subscript
166 zero denotes values at ambient condition) when its pressure derivative K' is fixed at 4.
167 This result is in good agreement with the present calculation (Table 3) and previous
168 theoretical calculations (K_0 = 252, K' = 4.26 by Karch et al. 1996; K_0 = 240, K' = 3.63
169 by Durandurdu 1996). Experimental P-V data are bracketed by LDA and GGA EoSs at
170 300 K; GGA volume is larger than LDA. The present experimental P-V data for the
171 ZB-type SiC are also plotted in Figure 4. They are consistent with the EoS previously
172 reported by DAC experiments (Yoshida et al. 1993).

Our experiments demonstrate that volume reduction associated with the ZB to RS transition is 17.3 % (Figure 4), consistent with the present GGA and LDA calculations. Such a large volume reduction has been found for similar ZB–RS transitions in other materials such as CdTe (ΔV = 16.5 %) (Onodera 1969b), ZnS (15.6 %) (Bilge et al. 2008), and BeO (11.1 %) (Sahariah and Ghosh 2010).

DISCUSSION

The present high *P-T* DAC experiments showed that the ZB–RS transition in SiC occurred at 74 GPa and 2100 K (Figure 3). The higher transition pressure reported by Yoshida et al. (1993) is likely due to kinetic hindering of the phase transition, considering the fact that their experiments were made at room temperature without heating. Indeed, as described above, our XRD data found that the starting 6*H* structure was preserved without any changes when heated to 2200 K for 2 min around 90 GPa. Such a kinetic effect may have extended to the shock-wave experiments by Sekine and Kobayashi (1997) as well, who also found a solid–solid phase transition above 100 GPa.

The *P-T* conditions of the ZB–RS transition observed in the present experiments are far beyond the phase boundaries we calculated using both LDA and GGA. Instead, they

190 are located between the two boundaries calculated in this study using GGA and by Catti
191 (2001) using B3LYP functional (Figure 3). B3LYP is one of the hybrid XC functionals
192 which partly take the exact electronic exchange into account. The present study suggests
193 that, in SiC, partial inclusion of exact electronic exchange into XC functional might be
194 important to calculate relative energy between phases with considerably different bond
195 lengths. On the other hand, B3LYP certainly overestimates the transition pressure,
196 indicating the necessity of using a more appropriate XC functional (e.g., to deal
197 explicitly with the kinetic energy density—meta-GGA— or van der Waals interaction)
198 to calculate the transition pressure precisely.

199 The Clapeyron slope of the ZB–RS boundary is not well constrained in the present
200 experiments, but is estimated to be -1.3 MPa/K at 500 K, -2.6 MPa/K at 1000 K, and
201 -4.0 MPa/K at 2000 K from our GGA calculations (Figure 3); it becomes larger as
202 temperature increases. A similar magnitude of negative Clapeyron slope (-1.2 to -1.5
203 MPa/K) has been determined for the ZB–RS transition in CdSe and CdTe with an
204 almost identical volume change (17 to 20 %) below 3.5 GPa and 800 K (Onodera 1969a,
205 b).

206

207 **IMPLICATIONS**

These results suggest that SiC, one of the main constituents in carbon-rich exoplanets (Madhusudhan et al. 2012; Wilson and Militzer 2014), undergoes a phase transition from the ZB to the RS structure around 70 GPa depending on the thermal structure. It forms a major boundary at certain depths inside carbon-rich planets, across which density increases by 21 %. Since this phase transition has a large negative Clapeyron slope with such a great volume change, it potentially affects thermal convection in their interiors. SiC is known to be very rigid and thermally conductive. The hardness of the high-pressure polymorph of SiC, the RS-type phase, is not known but is likely harder than low-pressure phases because a material with higher bulk modulus usually exhibits larger hardness (see a review by Haines et al. 2001). Its thermal conductivity is 270 W/m/K at ambient conditions; much higher than the 85 W/m/K for metallic Fe and the 5 W/m/K for Mg_2SiO_4 olivine (Hofmeister 1999), although it is reduced remarkably by small amounts of impurities. It is therefore unlikely that thermal convection takes place in an SiC layer as long as it is almost pure or mixed with carbon. Nevertheless, it is also possible that SiC coexists with silicate materials, even in the interior of 55 Cancri e (Madhusudhan et al. 2012), depending on the C/O ratio of the planetary system and the orbital separation during condensation (Bond et al. 2010). The effective viscosity of SiC + silicate mixture can diminish

226 substantially when the weaker silicate forms interconnected networks (see Yamazaki
227 and Karato 2001 for $MgSiO_3$ bridgmanite + MgO ferropericlase mixture). The
228 conductivity also drops when SiC grains are isolated in a silicate matrix. Therefore,
229 when smaller amounts of SiC are mixed with silicate, thermal convection possibly
230 occurs inside carbon-rich planets, and the ZB–RS boundary limits vertical material
231 transport and separates convection layers.

232

233 **ACKNOWLEDGMENTS**

234 We thank Y. Nakajima and R. Sinmyo for their support and advice during
235 high-pressure experiments. Synchrotron XRD measurements were made at BL10XU,
236 SPring-8 (proposals 2015A0080 and 2015B0080). Comments from two anonymous
237 reviewers were valuable to improve the manuscript.

238

REFERENCES CITED

Baroni, S., de Gironcoli, S., Dal Corso, A., and Giannozzi, P. (2001) Phonons and related crystal properties from density-functional perturbation theory. Reviews of Modern Physics, 73, 515.

Blige, M., Kart, S.Ö., Kart, H.H., and Cagin, T. (2008) B3–B1 phase transition and pressure dependence of elastic properties of ZnS. Materials Chemistry and Physics, 111, 559–564.

Bond, J.C., O'Brien, D.P., and Lauretta D.S. (2010) The compositional diversity of extrasolar terrestrial planets: I. in-situ simulations. The Astrophysical Journal, 715, 1050–1070.

Catti, M. (2001) Orthorhombic intermediate state in the zinc blende to rocksalt transformation path of SiC at high pressure. Physical Review Letters, 87, 035504.

Chang, K.J., and Cohen, M.L. (1987) Ab initio pseudopotential study of structural and high-pressure properties of SiC. Physical Review B, 35, 8196.

Durandurdu, M. (2004) Pressure-induced phase transition of SiC. Journal of Physics Condensed Matter, 16, 4411–4417.

Fei, Y., Ricolleau, A., Frank, M., Mibe, K., Shen, G., and Prakapenka, V. (2007) Toward

an internally consistent pressure scale. Proceedings of the National Academy of Sciences of the United States of America, 104, 9182–9186.

Giannozzi, P., et al. (2009) Quantum ESPRESSO: a modular and open-source software project for quantum simulations of materials. Journal of Physics Condensed Matter, 21, 395502.

Giannozzi, P., de Gironcoli, S., Pavone, P., and Baroni, S. (1991) Ab initio calculation of phonon dispersions in semiconductors. Physical Review B, 43, 7231.

Haines, J., Léger, JM., and Bocquillon, G. (2001) Synthesis and design of superhard materials. Annual Review of Materials Research, 31, 1–23.

Hofmeister, A.M. (1999) Mantle values of thermal conductivity and the geotherm from phonon lifetimes. Science, 283, 1699–1706.

Jepps, N.W., and Page, T.F. (1983) Polytypic transformations in silicon carbide. Progress in Crystal Growth and Characterization, 7, 259–307.

Karch, K., Bechstedt, F., Pavone, P., and Stauch, D. (1996) Pressure-dependent properties of SiC polytypes. Physical Review B, 53

Madhusudhan, N., Lee, K.K.M., and Mousis, O. (2012) A possible carbon-rich interior in super-Earth 55 Cancri e. The Astrophysical Journal Letters, 759, L40.

Miao, M.S., and Lambrecht, W.R.L. (2003) Unified path for high-pressure transitions of

SiC polytypes to the rocksalt structure. Physical Review B, 68, 092103.

Onodera, A. (1969a) High pressure transition in cadmium selenide. The Review of Physical Chemistry of Japan, 39, 65–77.

Onodera, A. (1969b) High pressure transition in cadmium telluride. The Review of Physical Chemistry of Japan, 39, 78–92.

Ozawa, H., Hirose, K., Yonemitsu, K., and Ohishi, Y. (2016) High-pressure melting experiments on Fe–Si alloys and implications for silicon as a light element in the core. Earth and Planetary Science Letters, 456, 47–54.

Perdew, J.P., and Zunger, A. (1981) Self-interaction correction to density-functional approximations for many-electron systems. Physical Review B, 23, 5048.

Perdew, J.P., Burke, K., and Ernzerhof, M. (1996) Generalized gradient approximation made simple. Physical Review Letters, 77, 3865; Erratum Physical Review Letters, 78, 1396 (1997).

Sahariah, M.B., and Ghosh, S. (2010) Dynamical stability and phase transition of BeO under pressure. Journal of Applied Physics, 107, 083520.

Sarasamak, K., Kulkarin, A.J., Zhou, M., and Limpijumnong, S. (2008) Stability of wurtzite, unbuckled wurtzite, and rocksalt phases of SiC, GaN, InN, ZnO, and CdSe under loading of different triaxialities. Physical Review B, 77, 02414.

Sata, N., Shen, G., Rivera, M.L., and Sutton, S.R. (2002) Pressure-volume equation of state of the high pressure B2 phase of NaCl. Physical Review B, 65, 104114.

Sata, N., Hirose, K., Shen, G., Ohishi, Y., and Hirao, N. (2010) Compression of FeSi, Fe_3C, $Fe_{0.95}O$, and FeS under the core pressure and implication for light element in the Earth's core. Journal of Geophysical Research, 115, B09204.

Sekine, T., and Kobayashi, T. (1997) Shock compression of 6H polytype SiC to 160 GPa. Physical Review B, 55, 8034.

Seto, Y., Nishio-Hamane, D., Nagai, T., and Sata, N. (2010) Development of a software suite on X-ray diffraction experiments. The Review of High Pressure Science and Technology, 20, 269–276.

Vanderbilt, D. (1990) Soft self-consistent pseudopotentials in a generalized eigenvalue formalism. Physical Review B, 41, R7892.

Wallace, D. (1972) Thermodynamics of Crystals. John Wiley, Hoboken, N.J.

Wilson, H.F., and Militzer, B. (2014) Interior phase transformations and mass-radius relationships of silicon-carbon planets. The Astrophysical Journal, 793, 34.

Yoshida, M., Onodera, A., Ueno, M., Takemura, K., and Shimomura, O. (1993) Pressure-induced phase transition in SiC. Physical Review B, 48, 10587.

310 **Figure captions**

311 **FIGURE 1.** Crystal structures of SiC in zinc-blende (ZB) and rock-salt (RS)-type
312 structures.

313

314 **FIGURE 2.** Changes in XRD patterns upon heating. Data were collected at (**a, f**) 56
315 GPa and (**b, g**) 58 GPa and 300 K before and after heating to 2060 K, respectively,
316 showing the formation and growth of the ZB phase. The ZB 111 and 220 lines
317 overlapping with 6*H* 012 and 110, respectively, became dotty and stronger after heating,
318 while the other 6*H* peak of 011 diminished. Patterns collected after further compression
319 at (**c**) 67 GPa and 300 K before the next heating cycle, (**d**) 92 GPa and 2610 K, and (**e**)
320 91 GPa and 2590 K demonstrating the appearance and growth of the RS phase. See text
321 for details.

322

323 **FIGURE 3.** Stability of ZB (closed symbols) and RS (open symbols) structures at high
324 *P*-*T* determined in the present XRD measurements. Solid curves with small circles were
325 the boundaries obtained by GGA and LDA calculations in this study. Broken curves
326 indicate the previous prediction using B3LYP functional (Catti, 2001) (gray),

considering the same negative temperature effect as GGA. We also drew a broken curve (red) that is consistent with the present experimental results.

FIGURE 4. *P–V* data for ZB (closed symbols) and RS (open symbols) structures of SiC at 300 K, with bold compression curves from Yoshida et al. (1993) and this study, respectively. Present calculations by GGA and LDA are also shown. The volume reduction at the phase transition is 17.3 %.

This is a preprint, the final version is subject to change, of the American Mineralogist (MSA)
Cite as Authors (Year) Title. American Mineralogist, in press.
(DOI will not work until issue is live.) DOI: http://dx.doi.org/10.2138/am-2017-6033

TABLE 1. Stabilities of zinc-blende and rock-salt types SiC

Run #	*P* (GPa)[a]	*T* (K)[b]	Duration (min)	Stable Structure	criteria[c]
1	67.6(23)	2060	5	Zinc-blende	1, 2
	92.3(30)	2610	2	Rock-salt	1
	91.3(30)	2590	4	Rock-salt	3
2	85.6(30)	2690	2	Rock-salt	1
	85.2(26)	2250	19	Rock-salt	3
	58.7(19)	1640	5	Zinc-blende	1
	62.6(22)	1960	1	Zinc-blende	3
3	75.1(24)	2120	20	Rock-salt	1
	78.7(28)	2590	1	Rock-salt	3
4	76.7(23)	2010	15	Rock-salt	2
5	63.9(27)	2720	1	Zinc-blende	1
	69.6(31)	3060	2	Zinc-blende	3
	81.2(31)	2910	1	Rock-salt	1
6	72.4(23)	2060	13	Zinc-blende	3

[a] Numbers in parentheses indicate uncertainty in the last digit.

[b] Temperature uncertainty is ±10%.

[c] Criteria for phase stability; 1) the appearance of new diffraction peaks, 2) grain growth inferred from spotty peaks in two-dimensional XRD image, and 3) the growth and reduction of the relevant peaks when both phasescoexisted in the XRD pattern.

This is a preprint, the final version is subject to change, of the American Mineralogist (MSA)
Cite as Authors (Year) Title. American Mineralogist, in press.
(DOI will not work until issue is live.) DOI: http://dx.doi.org/10.2138/am-2017-6033

TABLE 2. Unit-cell volume of SiC phases at 300 K

Run #	P (GPa)[a]	V (cc/mol)[b]
Zinc-blende-type		
2	68.7(5)	10.12(2)
	69.5(6)	10.11(1)
	69.8(8)	10.12(2)
	70.3(3)	10.14(2)
5	56.5(7)	10.37(1)
7	78.3(8)	9.92(5)
Rock-salt-type		
2	68.2(5)	8.37(1)
	69.5(6)	8.34(1)
	69.8(8)	8.34(1)
	70.3(3)	8.35(1)
3	50.1(2)	8.68(2)
5	63.9(4)	8.47(1)
	64.2(6)	8.43(1)
7	75.6(2)	8.28(1)
	93.0(7)	7.98(1)
	95.2(10)	7.95(1)
	97.5(9)	7.90(2)

Numbers in parentheses indicate uncertainty in the last digit.

[a] Based on the EoS of NaCl (Sata et al. 2002).

This is a preprint, the final version is subject to change, of the American Mineralogist (MSA)
Cite as Authors (Year) Title. American Mineralogist, in press.
(DOI will not work until issue is live.) DOI: http://dx.doi.org/10.2138/am-2017-6033

TABLE 3. Elastic parameters for SiC

Phase		V_0 (cm^3/mol)	K_0 (GPa)	K_0'
Zinc-blende-type	Experiment (Yoshida et al. 1993)	12.47	260(9)	2.9(3)
	LDA static	12.19	228.6	3.71
	GGA static	12.71	214.6	3.72
	LDA 300 K	12.29	223.4	3.71
	GGA 300 K	12.83	209.4	3.73
Rock-salt-type	Experiment (this study)	10.17(6)	235(9)	4(fixed)
	LDA static	9.7	270.8	4.03
	GGA static	10.14	256.9	3.95
	LDA 300 K	9.88	252.4	4.1
	GGA 300 K	10.32	241.3	3.99

Numbers in parentheses indicate uncertainty in the last digit.

This is a preprint, the final version is subject to change, of the American Mineralogist (MSA)
Cite as Authors (Year) Title. American Mineralogist, in press.
(DOI will not work until issue is live.) DOI: http://dx.doi.org/10.2138/am-2017-6033

(a) Zinc-Blende

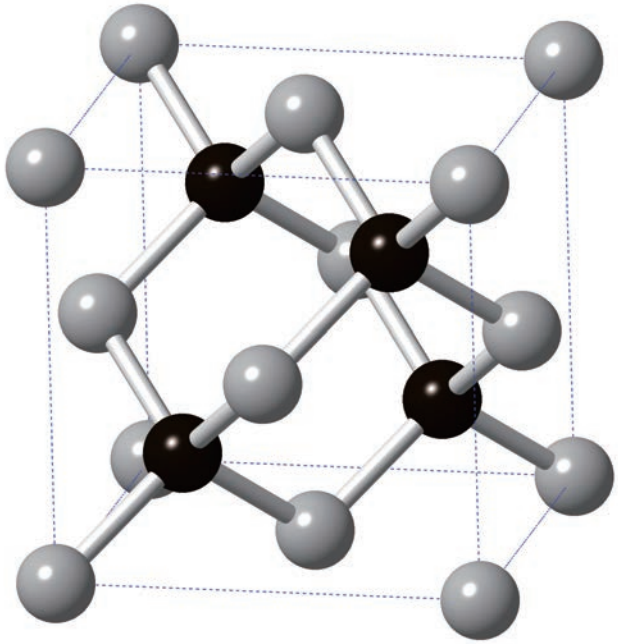

(b) Rock-salt

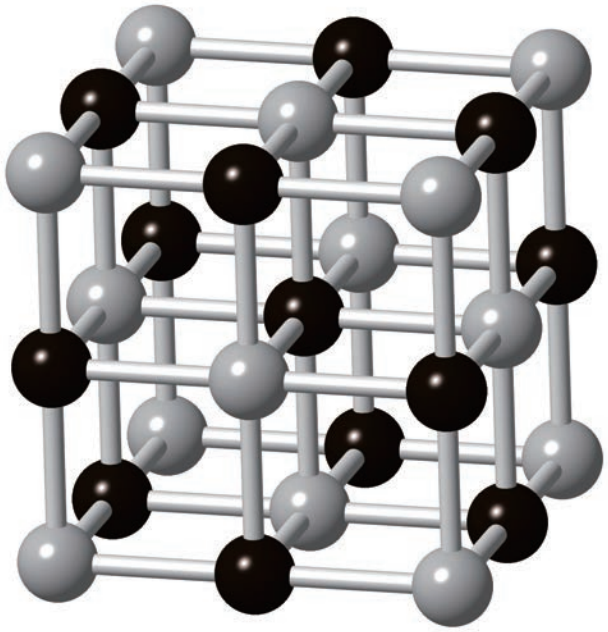

Fig. 1

This is a preprint, the final version is subject to change, of the American Mineralogist (MSA)
Cite as Authors (Year) Title. American Mineralogist, in press.
(DOI will not work until issue is live.) DOI: http://dx.doi.org/10.2138/am-2017-6033

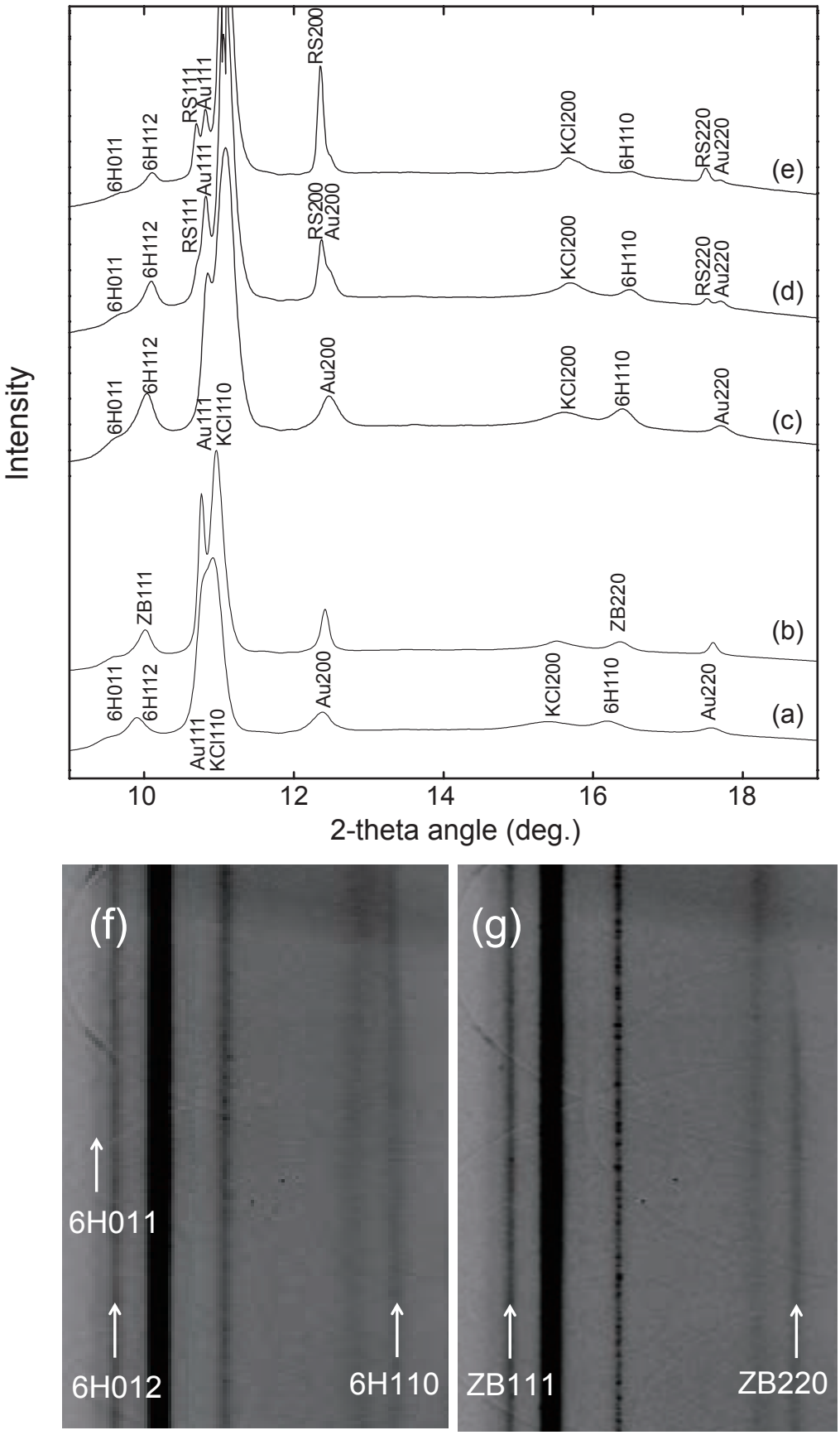

Fig. 2

This is a preprint, the final version is subject to change, of the American Mineralogist (MSA)
Cite as Authors (Year) Title. American Mineralogist, in press.
(DOI will not work until issue is live.) DOI: http://dx.doi.org/10.2138/am-2017-6033

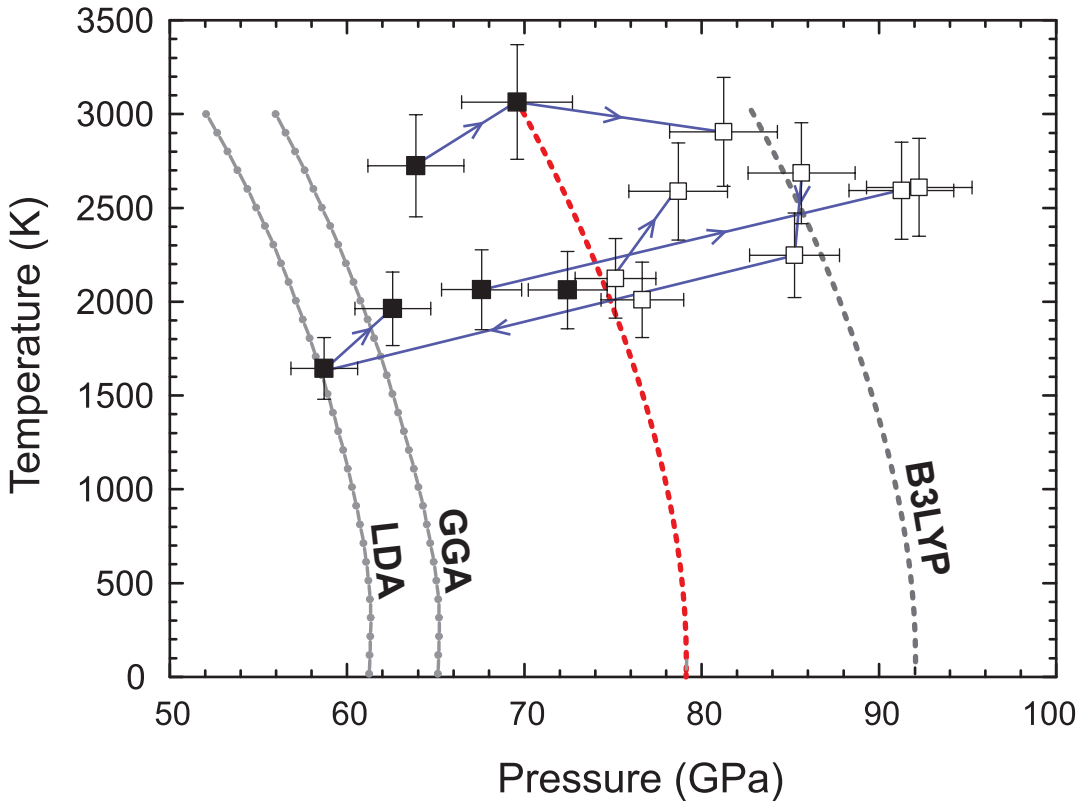

Fig. 3

This is a preprint, the final version is subject to change, of the American Mineralogist (MSA)
Cite as Authors (Year) Title. American Mineralogist, in press.
(DOI will not work until issue is live.) DOI: http://dx.doi.org/10.2138/am-2017-6033

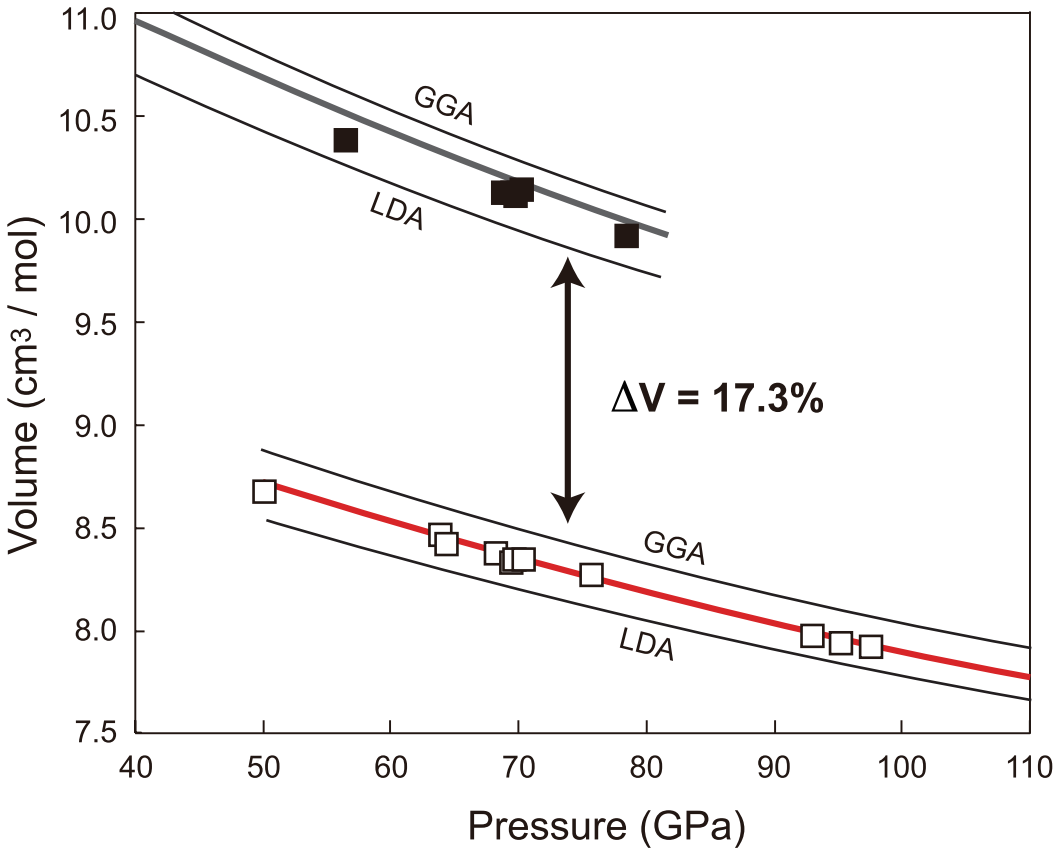

Fig. 4